The effect of annealing on structural and optical properties of ZnO thin films grown by pulsed filtered cathodic vacuum arc deposition

2006 J. Phys.: Condens. Matter 18 6391

(http://iopscience.iop.org/0953-8984/18/27/021)

INSTITUTE OF PHYSICS PUBLISHING JOURNAL OF PHYSICS: CONDENSED MATTER

J. Phys.: Condens. Matter **18** (2006) 6391–6400 doi:10.1088/0953-8984/18/27/021

The effect of annealing on structural and optical properties of ZnO thin films grown by pulsed filtered cathodic vacuum arc deposition

Ebru Şenadım, Hamide Kavak and Ramazan Esen

Faculty of Science and Letters, Department of Physics Adana, Cukurova University, 01330, Turkey

Received 28 April 2006
Published 23 June 2006
Online at stacks.iop.org/JPhysCM/18/6391

Abstract

Thin ZnO films were deposited at room temperature on glass substrates by a pulsed filtered cathodic vacuum arc deposition system. The crystallographic structure and the size of the crystallites in the films were studied by means of x-ray diffraction. These measurements show that all the films are crystallized in the wurtzite form, present in a preferred orientation along the (002) direction, and the grain size is estimated to be 18.9–42 nm. The crystallite sizes were found to increase and the x-ray diffraction patterns were sharpened by annealing. Optical properties of the ZnO films were studied using a UV–visible spectrometer and calculations made using the envelope method. The absorption coefficient and optical band gap of the films were increased while the refractive index was decreased by annealing. The best annealing temperature for pulsed cathodic vacuum arc deposition grown ZnO thin films on glass substrates was found to be 600 °C from optical properties. This temperature is as high as can be measured for glass substrates samples because of the glass properties.

1. Introduction

Zinc oxide (ZnO) is a very attractive material for application in optical devices such as blue, violet and ultraviolet (UV) light emitting diodes (LEDs) and laser diodes (LDs), since it has a direct and wide band gap of 3.3 eV at room temperature [1, 2]. Moreover, owing to the large exciton binding energy (∼60 meV), ZnO thin films exhibit very strong emissions caused by excitons even at room temperature [3]. In order to obtain high quality ZnO films, many growth techniques such as sputtering [4], pulsed laser deposition [5], MBE [6] and metal–organic chemical vapour deposition (MOCVD) [7] have been employed.

The pulsed cathodic vacuum arc deposition technique is new way to produce good quality (harder, denser and cleaner) thin films and coatings at low temperatures. The near 100% ionization of the cathode materials in the plasma means that the impact energy of the depositing ions at the growth surface can be readily controlled using electric fields. Their high energy plasma plume will readily ionize most background gases. These features make the pulsed

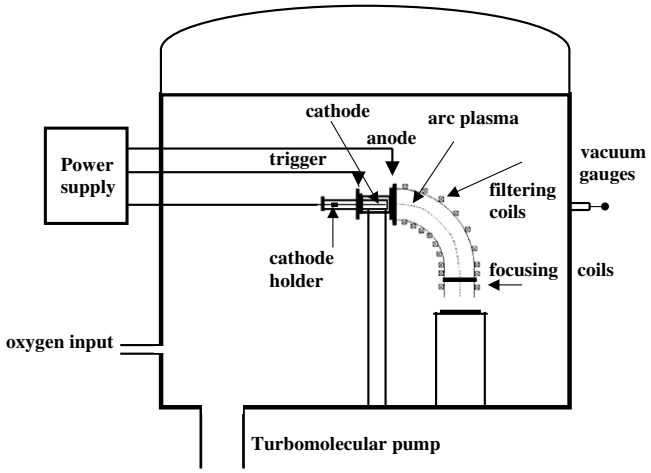

Figure 1. Schematic diagram of the pulsed filtered cathodic vacuum arc deposition system.

cathodic vacuum arc an ideal source for the production of metal oxides and nitrides [8]. Beside that, the pulsed filtered cathodic vacuum arc deposition (PFCVAD) technique is able to control the thickness at the atomic scale and there is no need to cool the system.

Thermal annealing is a method widely used to improve crystal quality and to study structural defects in materials. The structural and optical properties are crucial for semiconductor devices especially for light emitting devices. It is necessary to study how the properties are affected by thermal annealing. Thermal annealing is also used to activate dopants in semiconductors.

This paper reports the growth of ZnO films on glass substrates by the pulsed filtered cathodic vacuum arc deposition method. The influence of thermal annealing on the structural and optical properties of PFCVAD ZnO films is studied: in particular, the x-ray diffraction, transmittance, refractive index, energy band gap and absorption have been measured to observe the effect of the post-deposition annealing.

2. Experimental details

The PFCVAD system is schematically illustrated in figure 1. The cylindrical vacuum chamber was made of stainless steel (486 mm diameter and 385 mm in length) and evacuated using a primary and a turbomolecular pump (500 lt s^{-1}) to a base pressure below 1.3×10^{-8} Torr. The plasma source is a vacuum arc mini-gun (RHK Arc-20) consisting of a cathode, anode and focusing coil. An insulator ceramic separates the cathode structure from the anode, to which the positive terminal of the arc supply was connected, via the filter coil. The cathode of a vacuum arc is very active and evaporates ionized materials via the cathode spot, whereas the anode is usually inert and merely works as the acceptor of the evaporated materials emitted from the cathode spot. The arc was triggered by a 24 kV trigger pulse moved to cold emission by a trigger electrode inside a thick alumina tube which separates the anode and cathode. The arc was run in a repetitively pulsed mode with a pulse length of 60 μs. During deposition, a plasma beam with macroparticles and neutral atoms may be emitted from the cathodic arc process. Unwanted macroparticles and neutrals are then filtered out by the 90° curved solenoid filter. Only ions within a well-defined energy range are allowed to reach the substrate.

In this system, metallic zinc (1 mm in diameter and purity 99.99%) which was held in an alumina ceramic tube was employed as a cathode target, and oxygen (purity 99.9999%) was employed as the reactive gas. Films were deposited on ultrasonically cleaned glass substrates which were located 14 mm away from the anode. Oxygen gas was input into the chamber directly by a mass flow controller with constant flow rate of 135 sccm. The films were deposited under various conditions. The optimum deposition parameters were as follows: oxygen gas flow rate 135 sccm, fixed arc current 650 A, oxygen pressure 6.9×10^{-4} Torr and substrate temperature 25 °C. The distance from the target to the substrate was maintained at 14 mm.

The x-ray diffraction technique was used to specify the structural parameters, the phases present and the orientation of as-grown and annealed ZnO thin films. The x-ray diffraction measurements were performed using a Rigaku Miniflex x-ray diffraction system equipped with Cu Kα radiation of average wavelength 1.540 59 Å. All x-ray diffractograms were taken with the same parameters, such as 2θ between 20° and 70° and the scan speed of 2 °min^{-1}.

The optical properties of ZnO films deposited by PFCVAD were carried out with a double-beam spectrophotometer (Perkin-Elmer Lambda 2S) in the UV/visible/NIR regions. The optical transmittance at normal incidence was recorded in the wavelength range of 190–1100 nm. Swanepoel's envelope method was employed to evaluate optical constants such as the refractive index n and absorption coefficient α, from transmittance spectra. The thicknesses of the ZnO films were determined from interference fringes of transmission data measured over the visible range. And also a Filmetrics model F30 was employed to measure the thickness and refractive index of the ZnO films. The F30 is a spectral reflectance system that measures the thickness and optical constants of translucent thin film layers on opaque and transparent substrates. These results were consistent with the envelope method values.

3. Results and discussion

3.1. X-ray diffraction results

The crystalline quality and orientation of the ZnO thin films have been investigated by means of x-ray diffraction (XRD). Figure 2 shows the x-ray diffraction patterns of the ZnO (002) peaks of the as-deposited and annealed ZnO films. PFCVAD ZnO film was annealed in air at temperatures of 200, 300, 400, 500 and 600 °C with successive 1 h annealing times. The x-ray diffraction patterns are given in figure 2 for as-grown samples and ones annealed at five different annealing temperatures. The bottommost graph belongs to the as-grown ZnO sample and this is followed by that obtained after annealing at 200 °C for 1 h. The third line is obtained for the sample annealed at 300 °C for an additional 1 h and the next one following annealing at 400 °C for 1 h. Successive annealings at 500 and 600 °C, 1 h in each step, led to the fifth and six lines. The full width at half-maximum (FWHM) decreases with annealing treatment—from 0.46° to 0.021° after annealing—as given in table 1. That decrease is generally related to an improvement of the crystal quality of the ZnO films and to an enlargement of the grain size. These values are among the best reported values for ZnO thin films. The XRD patterns for the as-grown and the annealed ZnO films have a strong c-axis (002) orientation and the crystallinity of the film is improved by annealing. Even though the substrates were amorphous, 42 nm grain size was measured after annealing for 1 h at 600 °C.

The crystal lattice constant c and the interplanar distances of the diffracting planes d were identified using the Bragg equation $n\lambda = 2d \sin\theta$, where n is the order of the diffracted beam, λ is the wavelength of the x-ray and θ is the angle between the incoming x-ray and the normal of the diffracting planes. The values of c for as-deposited, 200, 300, 400, 500 and 600 °C

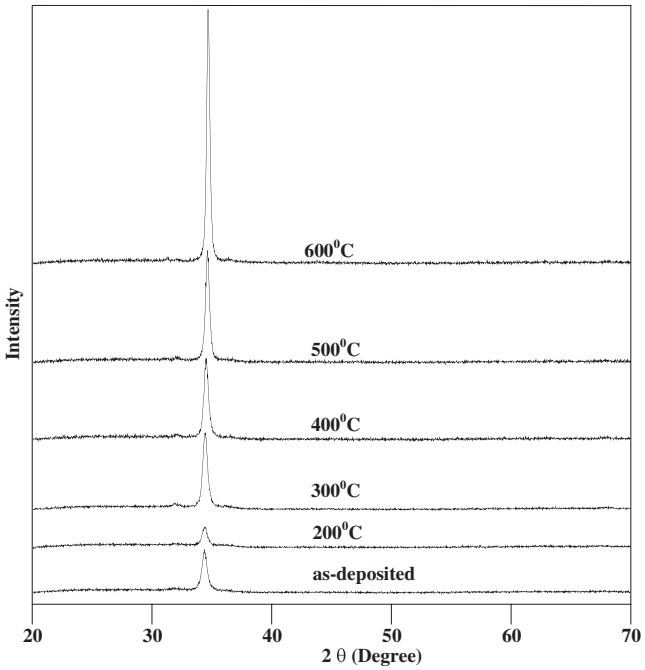

Figure 2. The XRD patterns of as-deposited and annealed ZnO films.

Table 1. X-ray diffraction data summary for 0.39 μm thick ZnO films grown by pulsed filtered cathodic vacuum arc deposition. (Note: H: hexagonal.)

Annealing temperature	Angle (2θ)	Relative peak intensity	Width (FWHM) (deg)	Remarks	Assignments	d (nm)	Grain size (D)
As-deposited	34.32	2 491.67	0.46	Sharp	(002)H	0.2610	18.9
200 °C	34.32	1 346.67	0.53	Broad	(002)H	0.2610	16.4
300 °C	34.38	4 146.67	0.41	Sharp	(002)H	0.2606	21
400 °C	34.50	4 403.33	0.37	Sharp	(002)H	0.2597	23.6
500 °C	34.60	5 936.67	0.25	Very sharp	(002)H	0.2590	29.1
600 °C	34.64	13 056.7	0.021	Very sharp	(002)H	0.2587	42

samples were 0.5220, 0.5220, 0.5212, 0.5194, 0.5180 and 0.5174 nm, respectively as reported in table 2.

The calculation of the film stress is based on the biaxial strain model. The strain $\varepsilon = \frac{c_{\text{film}} - c_{\text{bulk}}}{c_{\text{bulk}}}$ along the c-axis, i.e., perpendicular to the substrate surface, was calculated using XRD data (where c_{film} and c_{bulk} are the lattice parameter of the film and the strain-free lattice parameter of the ZnO thin films, respectively). The values of the strain for as-deposited and annealed ZnO thin films at 200, 300, 400, 500, 600 °C are given in table 2.

In order to understand the effect of the annealing on the stress of the ZnO thin film, the estimated values of the stress were calculated employing the following formula [9]:

$$\sigma = -233 \times 10^9 \left(\frac{c_{\text{film}} - c_{\text{bulk}}}{c_{\text{bulk}}} \right)$$

Table 2. Annealing effect on the lattice constant, strain and stress.

Annealing temperature	c (nm)	Strain (ε) ($\times 10^{-3}$)	Stress (σ) ($\times 10^{9}$ Pa)
As-deposited	0.5220	2.88	−0.67
200 °C	0.5220	2.88	−0.67
300 °C	0.5212	1.34	−0.31
400 °C	0.5194	−2.11	0.49
500 °C	0.5180	−4.80	1.11
600 °C	0.5174	−5.95	1.38

where c_{bulk} (0.5205 nm [10]) is the strain-free lattice constant. The stress of the ZnO thin films for as-deposited samples and ones annealed up to 300 °C was negative and at higher annealing temperatures it changed from negative to positive tensile. The stress values of as-deposited and annealed ZnO thin films are given in table 2.

The grain sizes of the crystallites were determined from x-ray diffraction data. The crystallite grain size D can be estimated using the Scherrer formula

$$D = \frac{0.9\lambda}{\beta \cos\theta}$$

where λ is the x-ray wavelength, θ is the Bragg diffraction angle, β is the FWHM in radians.

XRD analysis showed a shift toward higher degrees from 34.32 to 34.64 with annealing. So, one can attribute the increase of optical transmittance as the result of oxygen reaction with ZnO. The absorbed oxygen annihilates the oxygen vacancies, thus reducing the density of these donor-like defects and the carrier density [11]. Also, oxygen chemisorbs readily as an acceptor on ZnO surfaces [11–13] and pores in the films as O_2 by accepting an electron from the occupied conduction band state. Heating of the surface leads to desorption of oxygen with increase in the annealing temperature [14]. This may be the case for the degradation that appears at 200 °C annealing. The values of the peak position, peak intensity, FWHM, grain size and interplanar distance d for ZnO thin films are reported in table 1. These results indicate that the quality of the ZnO film was improved upon annealing.

3.2. Optical properties of PCVAD ZnO films

3.2.1. Transmittance measurements. The optical transmittance spectra of PCVAD ZnO films were measured with a double-beam spectrometer. From the interference fringes, the thickness d of the film was calculated using the following relation:

$$d = \frac{\lambda_1 \lambda_2}{2\left[n\left(\lambda_1\right)\lambda_2 - n\left(\lambda_2\right)\lambda_1\right]}$$

where $n(\lambda_1)$ and $n(\lambda_2)$ are the refractive indices at the two adjacent maxima (or minima) at λ_1 and λ_2. The zinc oxide film thicknesses were found to be 0.31–0.52 μm. The data presented are for a 0.39 μm thick ZnO sample and this value was verified with a Filmetrics F30 instrument.

The optical transmittance spectra of 0.39 μm thick ZnO films deposited on a glass substrate as grown and after annealing in air at several temperatures are shown in figure 3. After each step the optical transmittance of the sample was recorded and the annealing processes were carried out with the same sample, consecutively. The transmittance of the as-deposited ZnO film increased as the annealing temperature increased.

The maxima of the transmittances for all films are about 90% and 97%. After careful investigation of the maxima and lattice constant c, we find that the transmittance maxima of the

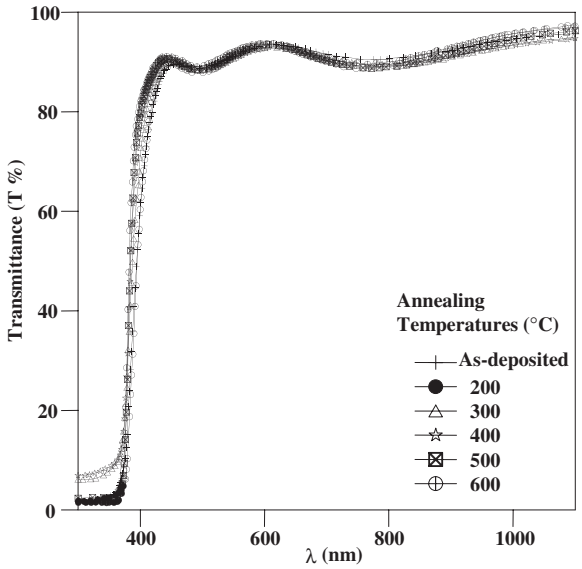

Figure 3. Transmittance spectra of ZnO films as deposited and after an annealing process.

samples decrease with increase of the lattice constant. Therefore, higher optical transmittance may be obtained by annealing during the growth process, which is suitable for growing ZnO transparent electrodes for solar cells.

3.2.2. Absorption coefficient and energy gap. The absorption coefficient α was calculated using

$$T = (1 - R)^2 \exp(-\alpha d)$$

where T is the transmittance of the thin film, R is the reflectance and d is the thickness of the film. Since the reflectivity is negligible and insignificant near the absorption edge, this relation simplifies to the following relation:

$$\alpha = \frac{1}{d}(2.3 * A)$$

where A is absorbance and d thickness of the film. The dependences of the absorption coefficient (α) on the wavelength for different values of the annealing temperature have been investigated, as shown in figure 4.

The optical energy band gap of ZnO films was determined from the optical absorption and transmission spectra. The relation between the absorption coefficient and the incident photon energy is given by [15–18]

$$\alpha h\nu = B(h\nu - E_g)^n$$

where B is a constant and E_g is the optical energy gap. For a direct transition a value of $n = \frac{1}{2}$ was found to be most suitable for ZnO thin film, since it gives the best linear graph in the band edge region. Figure 5 shows a plot of $(\alpha h\nu)^2$ versus $h\nu$ for as-deposited and annealed ZnO samples. The E_g value can be obtained by extrapolating the linear portion to the photon energy axis. The band edge sharpness was calculated using an $(\alpha h\nu)^2$ versus energy plot. The optical energy band gaps, band edge sharpness (B) and the absorption edges of ZnO samples as deposited and annealed at several temperatures are reported in table 3. The absorption edges

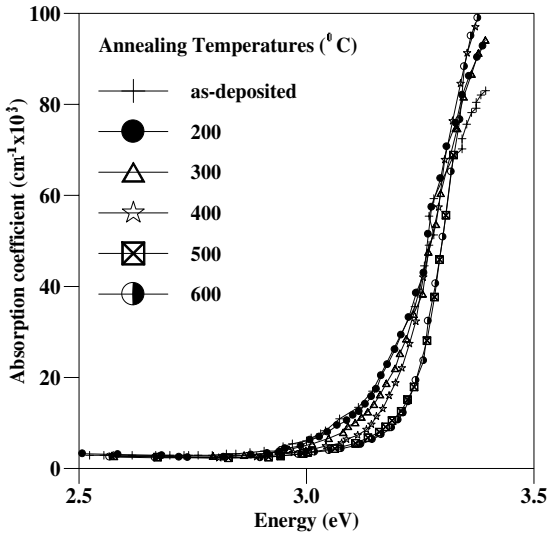

Figure 4. Absorption coefficients (α) as a function of photon energy $h\nu$ for as-deposited and annealed ZnO films.

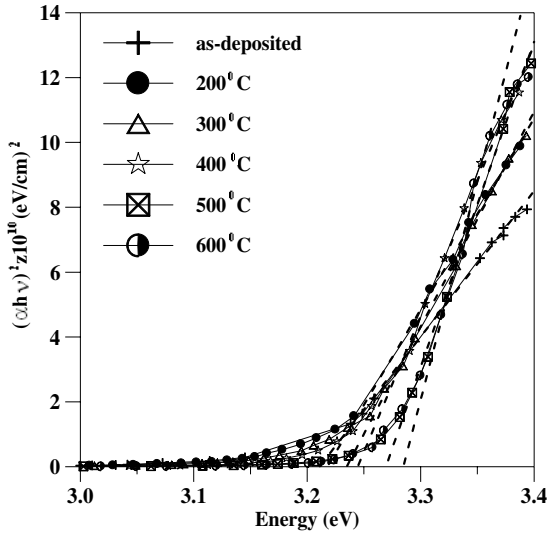

Figure 5. Plots of $(\alpha h\nu)^2$ versus $h\nu$ for as-deposited and annealed ZnO films.

move to lower wavelength values with increasing annealing temperature, as indicated in table 3. Figure 6 shows the evolution of the optical gap versus the annealing temperature. For the as-deposited films, E_g increases from 3.21 to 3.29 eV with increasing annealing temperature.

The dependence of the absorption coefficient (at $\lambda = 409$ nm) on the annealing temperature is also shown in figure 6. It is clear that the absorption coefficient decreases with increasing annealing temperature. The strong absorption and dispersion in the wavelength range indicates that the energy gap is located in that region, $\lambda < 388$ nm.

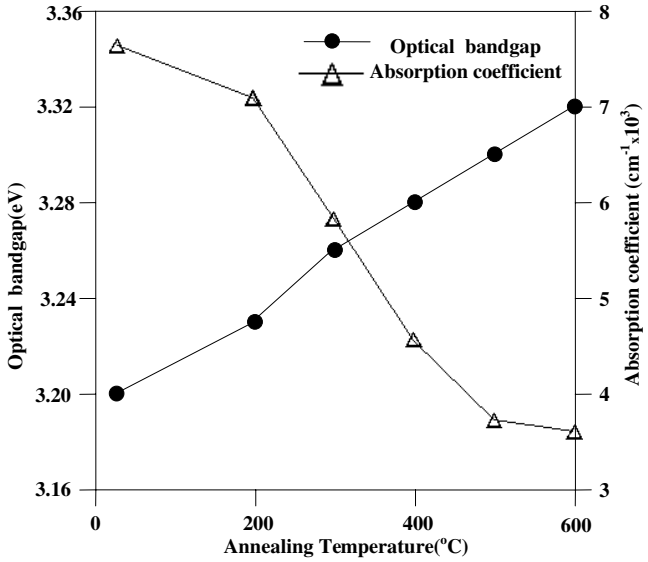

Figure 6. The dependence of the optical energy gap and absorption coefficients (at the wavelength of 409 nm) on the annealing temperature for ZnO thin film.

Table 3. The variation in optical band gap, refractive index, absorption edge and band edge sharpness with annealing temperature.

Annealing temperatures (°C)	Optical gap (eV)	Refractive index ($\lambda = 409$ nm)	Absorption edge (nm)	Band edge sharpness (10^9) (eV cm^{-2})
As-deposited	3.21	2.31	388	3.44
200	3.22	2.22	384	4.56
300	3.23	2.10	380	5.60
400	3.24	2.04	378	7.03
500	3.27	1.98	376	8.56
600	3.29	1.96	373	8.84

According to Gao [19] numerous factors influence the optical properties, such as the impurity concentration, oxygen or zinc vacancies and grain boundaries. With the use of the same target and the same gases, the impurity concentration in the coating must be maintained constant for all the series.

3.2.3. Refractive index. The refractive index (n) was determined using the well-known envelope method [20, 21]. For this purpose upper and lower envelopes of the transmittance curves were drawn in figure 3. The refractive index of the films was found using the following formula:

$$n = [N + (N^2 - n_s^2)^{1/2}]^{1/2}$$

$$N = \frac{(n_s^2 + 1)}{2} + 2n_s \frac{(T_{max} - T_{min})}{T_{max} T_{min}}$$

where n is the refractive index of the film, n_s is the refractive index of the glass substrate, T_{max} and T_{min} are the transmittance values for a given wavelength obtained from the envelope curves.

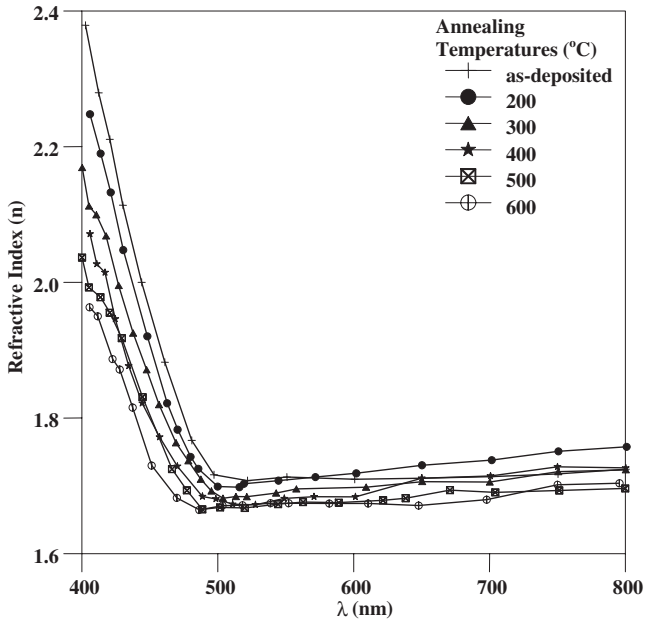

Figure 7. Wavelength dependence of the refractive index $n(\lambda)$ for as-deposited and annealed ZnO films.

The wavelength dependence of the refractive index $n(\lambda)$ for as-deposited and annealed ZnO samples in the visible region is shown in figure 7. The refractive index, n, experienced a noticeable decrease toward the end of the visible spectrum. The dependence of the refractive index n, for several wavelengths, on the annealing temperature is depicted in figure 8. It is observed that the value of n decreases as the annealing temperature increases up to 600 °C. The values of n, with the annealing temperatures, are also reported in table 3.

4. Conclusion

High quality zinc oxide thin films have been deposited on glass substrates by pulsed filtered cathodic vacuum arc deposition. Through XRD analysis, we have shown that the as-deposited thin films are highly oriented and just one peak, attributed to the (002) line of the hexagonal ZnO wurtzite phase, appears. When ZnO thin films are subjected to an annealing treatment in air, the crystallite sizes, intensity and angle increase; in contrast, the FWHM, interplanar distance d and lattice constant c decrease. We correlate these results with a possible increase in crystallinity and reduction in microvoids and oxygen absorption.

The optical energy gap was found to be affected by the annealing temperature. Films showed high values of the absorption coefficient for $\lambda < 385$ nm. The absorption coefficient has a high value for the as-deposited state, then decreases with increase in the annealing temperature. A rapid decrease of the refractive index n with increasing annealing temperature was found.

A decrease in peak height and an increase in the FWHM of the XRD pattern were observed at 200 °C for 1 h annealing. We propose that this degradation is probably due to desorption of trapped gases in the film and, when they leave the film, the number of microvoids in the film increases. For these reasons annealing at 200 °C for one hour has detrimental effects on the

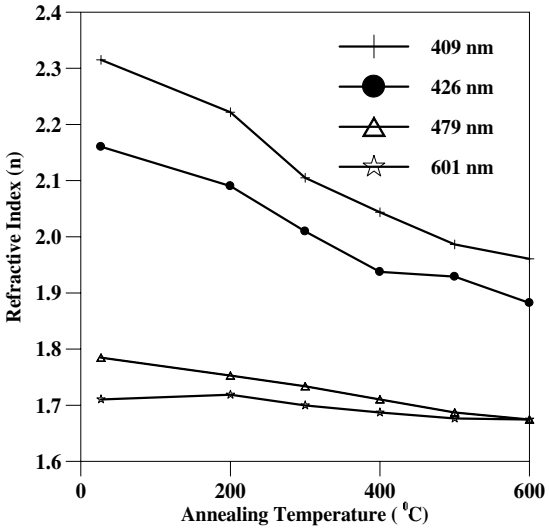

Figure 8. The dependence of the refractive index (n) at several wavelengths on the annealing temperatures for ZnO films.

films; further annealing at higher temperatures increases the crystallite sizes and reduces the stress between the substrate and films.

Acknowledgments

This work was supported by the Research Fund of University of Cukurova, Adana, Turkey (Project No. 2004K120360-1).

References

[1] Srikant V and Clarke D R 1998 *J. Appl. Phys.* **83** 5447
[2] Reynolds D C, Look D C, Jogai B and Morkoc H 1997 *Solid State Commun.* **101** 643
[3] Hummer K 1973 *Phys. Status Solidi* b **56** 249
[4] Jeong S H, Kim I S, Kim S S, Kim J K and Lee B T 2004 *J. Cryst. Growth* **264** 110
[5] Choi J H, Tabata H and Kawai T 2001 *J. Cryst. Growth* **226** 493
[6] Miyamoto K, Sano M, Kato H and Yao T 2004 *J. Cryst. Growth* **265** 34
[7] Munuera C, Zúñiga-Pérez J, Rommeluere J F, Sallet V, Triboulet R, Soria F, Muñoz-Sanjosé V and Ocal C 2004 *J. Cryst. Growth* **264** 70
[8] Anders S, Anders A, Rubin M, Wang Z, Raoux S, Kong F and Brown I G 1995 *Surf. Coat. Technol.* **76/77** 167
[9] Wang Y G, Lau S P, Lee H W, Yu S F, Tay B K, Zang X H, Tse K Y and Hng H H 2003 *J. Appl. Phys.* **94** 1597
[10] Puchert M K, Timbrell P Y and Lamb R N 1996 *J. Vac. Sci. Technol.* A **14** 2220
[11] Zhang D H and Brodie D E 1994 *Thin Solid Films* **238** 95
[12] Hirschwald W H 1985 *Acc. Chem. Res.* **18** 228
[13] Many A 1974 *CRC Crit. Rev. Solid State Sci.* **4** 515
[14] Tang W and Cameron D C 1994 *Thin Solid Films* **238** 83
[15] Tauc J 1974 *Amorphous and Liquid Semiconductors* ed J Tauc (New York: Plenum) p 159
[16] Urbach F 1953 *Phys. Rev.* **92** 1324
[17] Mott N F and Davis E A 1979 *Electronics Processes in Non-Crystalline Materials* (Oxford: Clarendon) p 428
[18] Oe K and Toyoshima Y 1973 *J. Non-Cryst. Solids* **58** 304
[19] Gao P, Meng L J, Dos Santos M P, Teixera V and Andritschky M 2000 *Vacuum* **56** 143
[20] Soliman L I and Ibrahim A M 1997 *Fizika* A **6** 181
[21] Won D J, Wang C H, Jang H K and Choi D J 2001 *Appl. Phys.* A **73** 595